Research Article | Vol. 29, No. 18 / 30 Aug 2021 / Optics Express 28359
Optics EXPRESS

Simple way to fabricate orderly arranged nanostructure arrays on diamond utilizing metal dewetting effect

TIAN-FEI ZHU,[1,2,*] YAN LIANG,[1,2] ZHANGCHENG LIU,[1,2] YAN-FENG WANG,[1,2] GUO-QING SHAO,[1,2] FENG WEN,[1,2] TAI MIN,[3] AND HONG-XING WANG[1,2]

[1]*Key Lab for Physical Electronics and Devices of the Ministry of Education, Faculty of Electronics and Information Engineering, Xi'an Jiaotong University, Xi'an 710049, China*
[2]*Institute of Wide Bandgap Semiconductors, Xi'an Jiaotong University, Xi'an 710049, China*
[3]*Spintronic Materials and Quantum Devices Research Center, Xi'an Jiaotong University, Xi'an 710049, China*
[*]*zhutianfei19@xjtu.edu.cn*

Abstract: We introduce a simple method with thermal annealing round gold disk for agglomeration to fabricate orderly arranged nanostructure arrays on diamond for single photon source applications. In the annealing process, the dependence of gold sphere size on disk thickness and diameter was investigated, showing that gold sphere diameter was decreased with decreasing gold disk thickness or diameter. The condition parameters of ICP etch were adjusted to obtain different nanostructure morphologies on diamond. The collection efficiency of nitrogen-vacancy (NV) center embedded in nanostructure as-fabricated could reach to 53.56% compared with that of 19.10% in planar case with the same simulation method.

1. Introduction

Color centers in diamond have been identified as excellent candidates for a wide range of applications such as optical quantum communication [1–2], quantum computation [3], biological detection [4–5] and high precision quantum sensor for electromagnetic field, temperature and pressure [6–8]. For single color center applications, enhancement of detected photon numbers is important for high performance of related devices. Optical nanostructures have abilities to enhance signals emitted from a single photon source in diamond due to their passive optical coupling and Purcell effect with color centers, which is an inevitable technique to realize applications mentioned above [9]. Diamond nanostructures include randomly and orderly arranged arrays have been reported with various routines [10–15]. For instance, nanopillars, nanocones and nanoneedle arrays were fabricated for NV center emission [16–18]. Besides, the gradually understood silicon-vacancy center, with its strong zero-phonon line (ZPL) transition, short excited-state lifetime and spectrally-narrow luminosity, also stands in need of nanostructure for improving photon emission [19,20]. Among them, many fabrication methods of orderly arranged nanostructure arrays rely on electron beam lithography (EBL) direct writing technique [13–14,17,18,21], which has limitations for efficient and scalable production. Although conventional technique such as photolithography can be utilized for industrial diamond microstructure manufacture, its resolution limits the structure size to micrometer scale. In addition, compared with micro-sized pattern, mask stripping of nano-pattern is more difficult. Improved method to scalable fabrication of diamond nanostructure arrays is expected.

In our work, we introduce a simple method with thermal annealing patterned gold disk for agglomeration to fabricate orderly arranged nanostructure arrays on diamond. Gold dot mask size dependence on size of photolithography pattern and diamond nanostructure shape dependence

#433037 https://doi.org/10.1364/OE.433037
Journal © 2021 Received 1 Jun 2021; revised 7 Aug 2021; accepted 8 Aug 2021; published 18 Aug 2021

Optics EXPRESS

on inductively coupled plasma (ICP) etch condition were investigated. Both micro- and nano-structures on diamond surface have been fabricated. The Finite Difference Time Domain (FDTD) simulations were carried out to study the emission performances of a NV center embedded in nanopillars with various morphologies.

2. Experimental

In our work, we use IIa type chemical vapor deposited (001) diamond with high quality for fabricating orderly arranged nanopillar arrays. The diamond samples are obtained by homogeneous growth on a HPHT diamond substrate measuring 3×3×0.4 mm^2 with our home-built equipment. During growing process, gas of O_2 was added to restrain defect formations. Figure 1 shows the fabrication flow chart. The SPR220 photoresist (PR) was spun on a cleaned diamond, resulting in a PR thickness of 3 μm. The standard photolithography process was used to form round hole pattern with diameter of 1-10 μm. Gold disks with thickness range from 10 to 230 nm were obtained with electron beam evaporation and lift-off processes. Then the samples were hold in a furnace for annealing at desired temperature for various time. During the annealing, gold disk with micro-size turned to be sphere with nanoscale size due to metal dewetting effect, which is etching mask for diamond nanostructures. Finally, the diamond with optimized gold dot arrays masks were ICP etched to obtain orderly arranged nanostrutures. Here, O_2 gas was used for etching gas with flow rate of 50 sccm. Chamber pressure and coil power were 10 mTorr and 450 W, respectively. Various platen powers ranged from 25 to 100 W were applied for different morphologies of nanostructures. The etching time ranged from 5 s to 3 min. After ICP etch, some samples were washed in aqua regia to remove remained gold. The morphologies of these nanostructures were characterized by scanning electron microscopy (SEM). The optical properties of as-fabricated diamond nanostructures with different shapes were investigated with FDTD Solutions software.

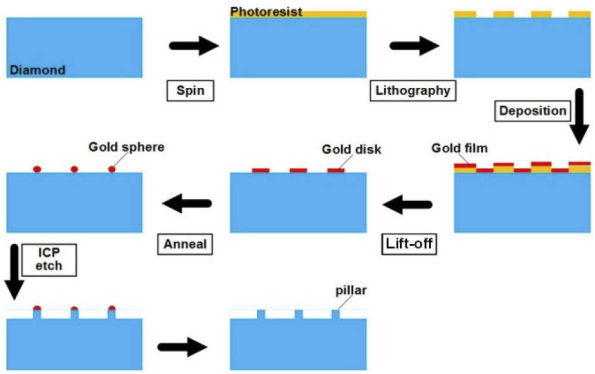

Fig. 1. Schematic of nanostructures fabrication on diamond surface.

3. Results and discussion

3.1. Preparation of gold sphere mask

To verify the hypothesis that gold disk can be assembled to a sphere dot by thermal annealing, round disks with diameter of 3, 5, 10 and 20 μm were annealed. Each disk has thickness of 230 nm and was annealed at 1100 °C for 5 min at vacuum ambient. Since gold is antioxidant and graphitization on diamond surface is easily etched off during etching process, a rough vacuum in furnace chamber was obtained using a mechanical pump and reached to about 5 Pa. Figure 2 shows SEM results of spheres obtained from gold disks with diameters of 3, 5, 10 and 20 μm,

Optics EXPRESS

respectively. All turned to be sphere shape, demonstrating that gold disk was dewetted and assembled to a sphere. From the results in Fig. 2, the disk edge profiles can be seen, whose diameter is close to that of gold disk. When the shape of disk was changed to sphere, the diameter of metal mask shrinks from micro to nano. This assembling phenomenon could be thought that gold turns to be sphere with tension force to keep surface energy minimum during annealing process.

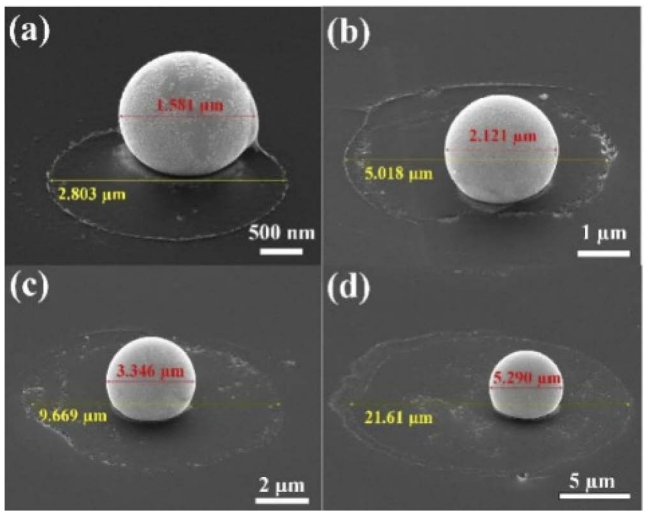

Fig. 2. SEM images of gold spheres after annealing of gold disk with diameter of (a) 3, (b) 5, (c) 10 and (d) 20 μm, respectively.

The relationship between sphere and disk diameter was illustrated shown in Fig. 3 indicated with circles. From the relation, the diameter of sphere increased with increasing disk diameter under the same gold film condition. The sphere diameter dependence on disk diameter may be due to that the gold volume almost is constant before and after thermal annealing. Volumes of sphere and disk were evaluated by the volume calculation formula (1) and (2), respectively.

$$V_{disk} = \frac{\pi}{4} D^2 h \tag{1}$$

$$V_{sphere} = \frac{\pi}{6} d^3 \tag{2}$$

In the formula (1) and (2), V_{disk} and V_{sphere} are the volume of gold disk and sphere respectively. The D and h are diameter and thickness of gold disk, respectively. The d is diameter of gold sphere. When h is fixed, the D and d have a power function relation. Here the power and h equal 2/3 and 0.23, respectively. The theoretic relation corresponds well with the experimental results shown in Fig. 3. The deviations of experimental results from theoretical values range from 2.36 to 7.78 percent. The experimental values of d are a little bigger than calculated results. It may be ascribed to that gold sphere is not complete sphere since the bottom of sphere which is contact with diamond surface is a plane.

Based on above results, sphere size can be precisely designed by adjusting the disk diameter. On the other hand, we try to reduce the thickness of disk (h) to obtain sphere with nanoscale diameter.

The 5 μm diameter disks with thickness of 50 and 100 nm were prepared and treated using the same conditions with that of above annealing. The results are shown in Fig. 4. When thickness of disk is 100 nm, a 1.667 μm thickness sphere formed. The value follows the rules of formula

Optics EXPRESS

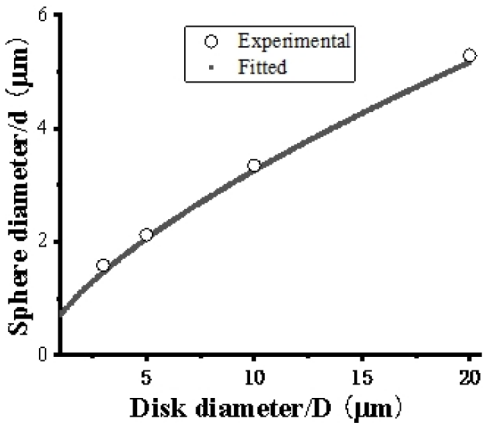

Fig. 3. Relation between sphere diameter (d) and that of disk (D) with experimental and theoretical results.

(1) and (2). In case of 50 nm thickness disk, no single gold sphere was formed in the inner region of the disk. Instead, randomly arranged nano gold spheres with various diameters were observed, which is similar to phenomenon observed in continuous film case in our previous work [22]. This demonstrates that the gold disk thickness is too thin to have enough surface tension force to gather a disk forming a complete sphere. Based on our results, in gold film case, the condition for forming a complete sphere should meet the requirement that the ratio of diameter to thickness is larger than 50 nm/5μm. Hence, a disk with both smaller diameter and thinner thickness was chosen to form a complete sphere. To obtain a nanopillar with size fitting for an NV center emission, a gold disk with diameter of 1 μm and thickness of 20 nm was annealed. With the formula (1) and (2), the theoretical value of sphere was calculated to be 310.7 nm. As shown in Fig. 5(b), the obtained gold sphere has diameter of about 334 nm, which comparable to theoretical value. The gold sphere arrays were used as a mask in next etch process.

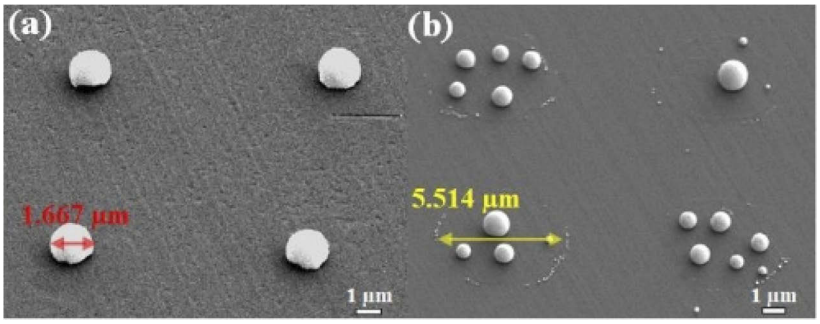

Fig. 4. SEM images of different thickness gold disk arrays with diameters of 5 μm after thermal annealing. Thickness of (a) 100 nm and (b) 50 nm.

3.2. ICP etch

Compared with mask of disk, sphere dot has curve surface which may have advantages in adjusting morphologies of diamond nanostructures. Diamond samples with gold dot arrays masks were etched under four different platen powers. The gold dots for all samples were prepared at the same experiment condition and have size of 334 nm. During ICP etch process, we chose various platen powers to etch diamond samples and other experiment conditions were fixed. As

Optics EXPRESS

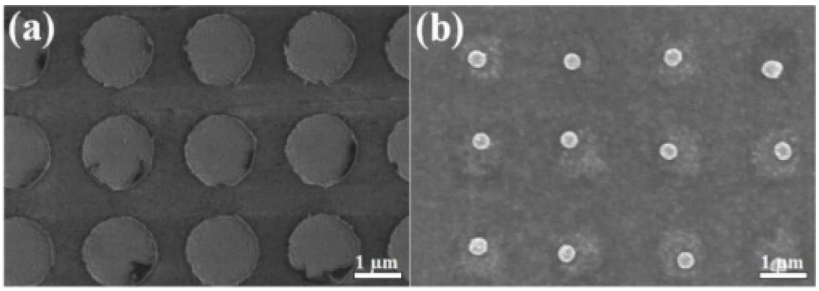

Fig. 5. Arrays of (a) disk with diameter of 1 μm and thickness of 20 nm and (b) sphere with diameter of 334 nm after thermal annealing.

shown in Fig. 6(a-d), pillars with different cone angles (CAs) were achieved under ICP condition of various powers. Their arrays are shown in Fig. 6(e-h), indicating a uniform morphology. With increased power, the obtained nanopillar has shaper tip and its CA decreased except the sample under power of 75 W. It could be thought that cover area of gold dot mask gradually decreased with etch time and a cone shape formed. When etch power increased, the cover area shrinks faster which causes a nanocone with smaller CA. The heights increase with increasing power, indicating that the etch rate of diamond increase with increasing power. Meanwhile, morphology of pillar in Fig. 6(d) is not smooth compared with others, suggesting that plasma energy is high to damage the surface of nanopillar under power of 100 W.

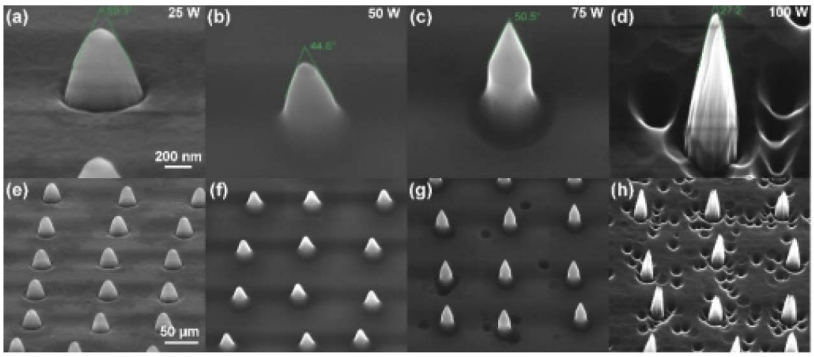

Fig. 6. SEM images of as-fabricated (a-d) nanostructures and (e-h) their arrays with gold dot masks under various power ICP conditions. (a, e) 25 W, (b, f) 50 W, (c, g) 75 W, (d, h) 100 W.

From these results, it can be found that the shapes of diamond nanostructures are easily adjusted by changing etch power with gold dots as mask.

3.3. Simulations

The emission from an NV center in diamond nanostructure as-fabricated was studied using FDTD simulations. To know the influence of nanostructures' CA on the emission efficiency of an NV center, nanopillars with CAs of 50.3°, 44.6° and 27.2° which are correspondence to experiment results and a fixed height of 600 nm were modeled. The NV center modeled as a s-polarized dipole was positioned in the middle point 20 nm below the tip. The simulated results are shown in Fig. 7. From Fig. 7(a-c), the optical field distributions of nanopillars with CAs of 50.3° and 44.6° are similar since the CAs are close to each other, and both exhibit different with that in nanopillar with CA of 27.2°, indicating that CA of nanopillar impacts the emission of an NV center.

Optics EXPRESS

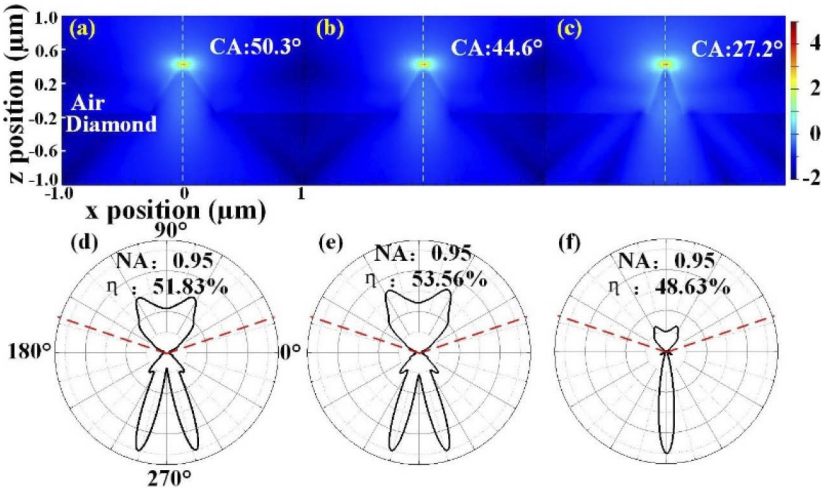

Fig. 7. FDTD simulation results of nanopillar with height of 600 nm and cone angles (CAs) of (a) 50.3°, (b) 44.6° and (c) 27.2°. Figure (a-c) and (e-g) share one coordinate axis, respectively. η represents collecting efficiency from a NV center using an objective with NA of 0.95.

Far field figures shown as Fig. 7(d-f) illustrate a clear sight of behavior that photon escapes from diamond. A microscope with a numerical aperture (NA) of 0.95 was modeled above samples to collect photons. The detecting region is area above red dash line indicated in Fig. 7(d-f). The photon collection efficiencies of nanopillars with CAs of 50.3°, 44.6°, and 27.2° were calculated to be 51.83, 53.56 and 48.63%, respectively. All nanostructures show abilities of increasing photo collection efficiencies compared to efficiency of 19.1% calculated in planar case. The results imply that efficiency of photo collection from a NV center embedded in nanopillar could be improved by adjusting the morphologies of nanopillar using the presented method.

Base on above, with conventional photolithography technique, orderly arranged nanostructures of diamond have been fabricated, suggesting a convenient way to obtain diamond nanostructures for single photon source applications. Furthermore, the patterned film annealing method is also applicable to nanostructure fabrication on other materials. This method has potential for fabricating nanostructures with sizes of 100 nm and even smaller since gold has large enough surface tension to form small masks during thermal annealing process. Instead of the point by point preparation of nanopatterns in electron beam lithography, nano-arrays pattern can be prepared by one-step exposure with photolithography. This method has advantages in mass production of nanostructure arrays.

4. Conclusions

Nanostructures have been fabricated on diamond using thermal annealing patterned gold film and ICP etching techniques. Gold sphere with nanoscale size could be obtained from gold disk with microscale size by thermal annealing. The nanoscale size of dot is dependent on film thickness and pattern size. Orderly arranged nano-dot arrays with size of 334 nm on diamond were obtained. By ICP etch, diamond nanostructure arrays were achieved. The shape of nanostructure could be adjusted by changing etch power. In combination with simulations, the as-fabricated nanostructure arrays have potential to improve photon collection efficiencies of single photo source from 19.10% in planar case to 53.56%.

Funding. Natural Science Basic Research Program of Shaanxi Province (2021GY223, 2021JQ056, 2021JQ062);

Optics EXPRESS

National Key Research and Development Program of China (2018YFE0125900); National Natural Science Foundation of China (61627812, 61804122, 62074127); China Postdoctoral Science Foundation (2019M660256, 2020M683485).

Disclosures. The authors declare that there are no conflicts of interest related to this article.

Data availability. Data underlying the results presented in this paper are not publicly available at this time but may be obtained from the authors upon reasonable request.

References

1. C. Kurtsiefer, S. Mayer, P. Zarda, and H. Weinfurter, "Stable Solid-State Source of Single Photons," Phys. Rev. Lett. **85**(2), 290–293 (2000).
2. N. Mizuochi, T. Makino, H. Kato, D. Takeuchi, M. Ogura, H. Okushi, M. Nothaft, P. Neumann, A. Gali, F. Jelezko, J. Wrachtrup, and S. Yamasaki, "Electrically driven single-photon source at room temperature in diamond," Nat. Photonics **6**(5), 299–303 (2012).
3. G. Waldherr, Y. Wang, S. Zaiser, M. Jamali, T. Schulte-Herbrüggen, H. Abe, T. Ohshima, J. Isoya, J. Du, P. Neumann, and J. Wrachtrup, "Quantum error correction in a solid-state hybrid spin register," Nature **506**(7487), 204–207 (2014).
4. L. T. Hall, G. C. G. Beart, E. A. Thomas, D. A. Simpson, L. P. McGuinness, J. H. Cole, J. H. Manton, R. E. Scholten, F. Jelezko, J. Wrachtrup, S. Petrou, and L. C. L. Hollenberg, "High spatial and temporal resolution wide-field imaging of neuron activity using quantum NV-diamond," Sci. Rep. **2**(1), 401 (2012).
5. L. Hanlon, V. Gautam, J. D. Wood, P. Reddy, M. S. Barson, M. Niihori, A. R. Silalahi, B. Corry, J. Wrachtrup, M. Sellars, V. Daria, P. Maletinsky, G. Stuart, and M. Doherty, "Diamond nanopillar arrays for quantum microscopy of neuronal signals," Neurophotonics **7**(03), 1 (2020).
6. L. Rondin, J. P. Tetienne, T. Hingant, J. F. Roch, P. Maletinsky, and V. Jacques, "Magnetometry with nitrogen-vacancy defects in diamond," Rep. Prog. Phys. **77**(5), 056503 (2014).
7. G. Kucsko, P. C. Maurer, N. Y. Yao, M. Kubo, H. J. Noh, P. K. Lo, H. Park, and M. D. Lukin, "Nanometre-scale thermometry in a living cell," Nature **500**(7460), 54–58 (2013).
8. M. W. Doherty, V. V. Struzhkin, D. A. Simpson, L. P. McGuinness, Y. Meng, A. Stacey, T. J. Karle, R. J. Hemley, N. B. Manson, L. C. L. Hollenberg, and S. Prawer, "Electronic Properties and Metrology Applications of the Diamond NV- Center under Pressure," Phys. Rev. Lett. **112**(4), 047601 (2014).
9. B. J. M. Hausmann, M. Khan, Y. Zhang, T. M. Babinec, K. Martinick, M. Mccutcheon, P. R. Hemmer, and M. Lončar, "Fabrication of diamond nanowires for quantum information processing applications," Diamond Relat. Mater. **19**(5-6), 621–629 (2010).
10. Z.C. Liu, T.F. Zhu, Y.F. Wang, I. Ahmed, Z. Liu, F. Wen, X. Zhang, W. Wang, S. Fan, K. Wang, and H.X. Wang, "Fabrication of Diamond Submicron Lenses and Cylinders by ICP Etching Technique with SiO_2 Balls Mask," Materials **12**(10), 1622 (2019).
11. J. Song, H. Li, F. Lin, L. Wang, H. Wu, and Y. Yang, "Plasmon-enhanced photoluminescence of Si-V centers in diamond from a nanoassembled metal–diamond hybrid structure," CrystEngComm **16**(36), 8356–8362 (2014).
12. Y. Zou, Y. Yang, W. Zhang, Y. Chong, B. He, I. Bello, and S. Lee, "Fabrication of diamond nanopillars and their arrays," Appl. Phys. Lett. **92**(5), 053105 (2008).
13. C. J. Widmann, C. Giese, M. Wolfer, D. Brink, N. Heidrich, and C. E. Nebel, "Fabrication and characterization of single crystalline diamond nanopillars with NV-centers," Diamond Relat. Mater. **54**, 2–8 (2015).
14. B. J. M. Hausmann, T. M. Babinec, J. T. Choy, J. S. Hodges, S. Hong, I. Bulu, A. Yacoby, M. D. Lukin, and M. Lončar, "Single Color Centers Implanted in Diamond Nanostructures," New J. Phys. **13**(4), 045004 (2011).
15. R. Nelz, J. Gorlitz, D. Herrmann, A. Slablab, M. Challier, M. Radtke, M. Fischer, S. Gsell, M. Schreck, C. Becher, and E. Neu, "Toward wafer-scale diamond nano- and quantum technologies," APL Mater. **7**(1), 011108 (2019).
16. T. M. Babinec, B. J. M. Hausmann, M. Khan, Y. Zhang, J. R. Maze, P. R. Hemmer, and M. Lončar, "A diamond nanowire single-photon source," Nat. Nanotechnol. **5**(3), 195–199 (2010).
17. S. Li, C. H. Li, B. W. Zhao, Y. Dong, C. C. Li, X. D. Chen, Y. S. Ge, and F. W. Sun, "A Bright Single-Photon Source from Nitrogen-Vacancy Centers in Diamond Nanowires," Chin. Phys. Lett. **34**(9), 096101 (2017).
18. L. Xie, T. X. Zhou, R. J. Stöhr, and A. Yacoby, "Crystallographic Orientation Dependent Reactive Ion Etching in Single Crystal Diamond," Adv. Mater. **30**(11), 1705501 (2018).
19. A. Sipahigil, K. D. Jahnke, L. J. Rogers, T. Teraji, J. Isoya, A. S. Zibrov, F. Jelezko, and M. D. Lukin, "Indistinguishable Photons from Separated Silicon-Vacancy Centers in Diamond," Phys. Rev. Lett. **113**(11), 113602 (2014).
20. S. Lagomarsino, A.M. Flatae, H. Kambalathmana, F. Sledz, L. Hunold, N. Soltani, P. Reuschel, S. Sciortino, N. Gelli, M. Massi, C. Czelusniak, L. Giuntini, and M. Agio, "Creation of Silicon-Vacancy Color Centers in Diamond by Ion Implantation," Frontiers in Physics 8, (2021).
21. D. J. McCloskey, N. Dontschuk, D. A. Broadway, A. Nadarajah, A. Stacey, J. P. Tetienne, L. C. L. Hollenberg, S. Prawer, and D. A. Simpson, "Enhanced Widefield Quantum Sensing with Nitrogen-Vacancy Ensembles Using Diamond Nanopillar Arrays," ACS Appl. Mater. Interfaces **12**(11), 13421–13427 (2020).
22. T.F. Zhu, Y. Liang, Z. Liu, J. Fu, Y. Wang, G. Shao, D. Zhao, J. Wang, R. Wang, Q. Wei, W. Wang, F. Wen, T. Min, and H.X. Wang, "Nanocone Structures Enhancing Nitrogen-Vacancy Center Emissions in Diamonds," Coatings **10**(6), 513 (2020).